Spectral dependence of third-order nonlinear optical properties in InN

H. Ahn, M.-T. Lee, and Y.-M. Chang

Citation: Applied Physics Letters **104**, 201904 (2014); doi: 10.1063/1.4878618
View online: http://dx.doi.org/10.1063/1.4878618
View Table of Contents: http://scitation.aip.org/content/aip/journal/apl/104/20?ver=pdfcov
Published by the AIP Publishing

Spectral dependence of third-order nonlinear optical properties in InN

H. Ahn,[a] M.-T. Lee, and Y.-M. Chang
Department of Photonics and Institute of Electro-Optical Engineering, National Chiao Tung University, Hsinchu 30010, Taiwan

(Received 17 April 2014; accepted 7 May 2014; published online 20 May 2014)

We report on the nonlinear optical properties of InN measured in a wide near-infrared spectral range with the femtosecond Z-scan technique. The above-bandgap nonlinear absorption in InN is found to originate from the saturation of absorption by the band-state-filling and its cross-section increases drastically near the bandgap energy. With below-bandgap excitation, the nonlinear absorption undergoes a transition from saturation absorption (SA) to reverse-SA (RSA), attributed to the competition between SA of band-tail states and two-photon-related RSA. The measured large nonlinear refractive index of the order of 10^{-10} cm^2/W indicates InN as a potential material for all-optical switching and related applications. © *2014 AIP Publishing LLC*.
[http://dx.doi.org/10.1063/1.4878618]

Indium nitride (InN) with a narrow direct bandgap ($E_G \sim 0.65$ eV) has superior electronic transport properties to other group-III nitrides so that InN has become attractive for various applications such as high-frequency electronic devices, near-infrared (NIR) optoelectronics,[1–5] and high-efficiency solar cells.[6] Because of its narrow bandgap, InN can be easily integrated with an optical fiber laser to achieve compact optical system. Recent dramatic increase of information transfer through internet requires switches operating at high rate for future telecommunication system. All-optical switching based on nonlinear optics may provide a solution for faster switches and the bandwidth of optical switch could reach beyond 1 THz unattainable by electronic switching techniques. In general, all-optical switching technology requires a nonlinear material with large nonlinear refraction (NLR) and small linear absorption. The InN film photoexcited at wavelength of 1550 nm shows the large optical bleaching and its recovery time can be less than a few picoseconds,[7] which makes InN an excellent candidate to realize all-optical switching for telecommunication systems.

Despite these prospects, studies on nonlinear phenomena of InN are scarce, and the reported results have been carried out only at several selected wavelengths, such as 800 nm and 1550 nm.[8–12] Moreover, the wide wavelength dependence near the bandgap has not been reported for InN. This is mainly due to the lack of suitable light sources as well as the detection systems in the NIR spectral range. Several contradictory results on the nonlinear absorption (NLA) referring to either saturation absorption (SA)[9,10] or reverse-SA (RSA)[8,12] for InN have been reported and the reported values of NLA coefficients vary widely in the range of 10^{-9}–10^{-6} cm/W.[8–12]

Here, we report the third-order nonlinearities of InN films grown by plasma-assisted molecular beam epitaxy (PAMBE). The Z-scan measurement[13] with femtosecond pulses in the wavelength range of 700–1600 nm allows the investigation of the nonlinear properties of InN epilayers near and below the bandgap energy. The wide spectral dependence of the nonlinear absorption cross-section (σ) is compared with the band-filling model, which is associated with the saturation of absorption for above-bandgap excitation. The transitional behavior of nonlinear absorption upon the increase of the wavelength and the intensity of excitation light demonstrates that there is absorption in the band-tail states for excitation photon energies below bandgap.

For this work, two *a*-plane InN epilayers were grown on *r*-plane $\{1\bar{1}02\}$ sapphire substrates by PAMBE. To improve the structural and electrical properties of InN films, a double buffer layer consisted of AlN/GaN (300/230 nm) was grown between the InN film and the substrate. And details of the growth procedure of *a*-plane InN films can be found elsewhere.[14] Since the optical absorption in InN films dramatically increases above the bandgap,[15] a thin InN epilayer with $d \sim 60$ nm (sample A) was prepared to study the non-resonant optical nonlinearity properties. We also prepared a thick sample (sample B) with $d \sim 1.4\,\mu$m for comparison. Figure 1(a) shows the photoluminescence (PL) spectra of samples A and B at room temperature. Despite being grown under similar conditions, samples A and B have different PL peak energies at ~0.76 and 0.65 eV, respectively. Table I shows that the carrier density of sample A measured by the Hall effect measurement is larger than that of sample B, indicating that the high PL peak energy in sample A can be attributed to the Moss-Burstein blue-shift in very thin films.[16] The back side of *r*-plane sapphire substrates was coated with a Ti layer for efficient and uniform heating during the PAMBE growth and before Z-scan measurement, Ti layer was removed by using a diluted HCl solution.

The Z-scan measurements were performed using a Ti:sapphire laser tunable in the range of 700-1080 nm and an optical parametric oscillator (OPO), providing tunability from 1100 nm to 1600 nm. Approximately, 120 fs-long pulses were focused at the sample surface, resulting in peak fluences in the range of 0.05–2 GW/cm^2. During the Z-scan measurements, samples are moved along the optical axis (*z*-direction) of the focused laser beam, while the transmittance of the sample is recorded as a function of the z-position. The estimated refractive index change of InN due to the cumulative thermal effect[17] is negligibly small (10^{-4}–10^{-5}) for our experiment. The Z-scan measurement

[a]Author to whom correspondence should be addressed. Electronic mail: hyahn@mail.nctu.edu.tw.

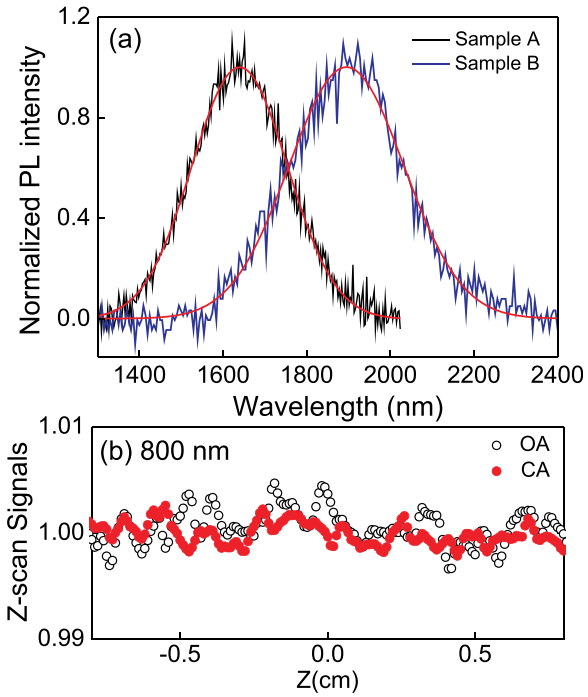

FIG. 1. (a) PL spectra from the InN films excited by femtosecond laser pulses at 800 nm. Sample A with a higher carrier density has a clearly blue shifted bandgap energy compared to sample B. (b) The OA and CA Z-scan signals measured at $\lambda = 800$ nm for the GaN/AlN buffer layer grown on a sapphire substrate.

from a sapphire substrate with a GaN/AlN buffer layer [Fig. 1(b)] shows no noticeable responses under the same excitation conditions adopted for the InN films. Similar responses are observed for other wavelengths used.

Figures 2(a) and 2(c) show the wavelength dependence of open-aperture (OA) Z-scan signals for samples A and B, respectively. The Z-scan signals from the thin InN layer in sample A are much smaller than those from the thick InN layer in sample B. The transmittance for the sample position far from the beam waist, where nonlinear effects are negligible, is normalized to unity. In Fig. 2(c), the transmitted Z-scan signal (ΔT) of sample B increases as the sample moves towards the focus and it reaches the maximum at the focus, exhibiting saturation of absorption. For sample B, the SA behavior is observed across the entire measured wavelength range and the peak value of ΔT ($\Delta T_{\max}$) continuously increases as the wavelength increases. The increase of $\Delta T_{\max}$ is also observed when the irradiance power is increased. In the case of sample A, SA-dominated Z-scan signals increase as the wavelength increases from 900 nm to 1200 nm. However, at ~1300 nm, a small valley within the peak appears near $z = 0$ and becomes deeper with the further increase of wavelength. The negative Z-scan signals attributed to RSA can also get significant as the pump fluence is increased, as shown in Fig. 2(b). In particular, the Z-scan signal measured at 0.5 GW/cm^2 in Fig. 2(b) shows the coexistence of SA and RSA.

TABLE I. Sample parameters of InN films measured by Hall effect measurement.

Sample	d (nm)	n ($\times 10^{19}$ cm^{-3})	μ (cm^2/V s)
Sample A	60	7.4	65.9
Sample B	1400	1.4	145.2

To fit the Z-scan data, we employ the standard Z-scan theory[13] with assumption of $\alpha(I) = \alpha_0 + \beta I$, where α, α_0, and β are the total, linear, and nonlinear absorption coefficients, respectively. The saturated absorption, especially near the bandgap energy, can be understood as the band-state filling by the photogenerated carriers, which relax rapidly to thermal distribution near the bottom of the conduction band. Therefore, large values of $\Delta T_{\max}$ at longer wavelengths in Fig. 2(c) are due to the smaller available states near the band edge. The change of the absorption coefficient due to photogenerated carriers is given by $\Delta\alpha = -\sigma\Delta N$, where σ is the nonlinear optical absorption cross-section and the density of photogenerated carriers $\Delta N\left(= \alpha_0 I_p \tau/\hbar\omega\right)$ is proportional to the absorbed light intensity. Here, τ is the temporal pulsewidth of laser beam, and I_p is the peak irradiance of the incident pulse. In the Z-scan measurement, the normalized transmittance is related to the sample position z by[13]

$$\Delta T(z) \propto \frac{-\alpha I_0 L_{eff}}{1 + z^2/z_0^2}, \tag{1}$$

where I_0 is the on-axis peak intensity at the focus, $L_{eff} = [1 - \exp(-\alpha_0 L)]/\alpha_0$ is the effective interaction length, L is the sample length, and the profile of the pulse has been assumed to be Gaussian. The Rayleigh diffraction length $z_0 \sim w_0^2/2$ is determined from the beam waist w_0 measured by the knife-edge method. Then, with the values of separately measured wavelength-dependent α_0,[15] the nonlinear optical absorption cross-sections are estimated from the best fitting curves shown in Fig. 2.

Figure 3 depicts the wavelength-dependent nonlinear optical absorption cross-sections measured from SA-induced Z-scan signals shown in Fig. 2. In the wavelength range between 1100 nm and 1300 nm, the measured absorption cross-sections are nearly identical for sample A and B, indicating that the SA behavior of InN films above the bandgap energy is not influenced by the film thickness. Here, the error bar is calculated from the laser intensity dependence of σ at a fixed wavelength. A drastic increase of σ with the increase of wavelength indicates the strong nonlinear absorption near the bandgap energy. This behavior can be understood by the band-filling model proposed by Miller *et al.*, in which the change of α near the bandgap energy is given by[18]

$$\Delta\alpha \approx A\left(\frac{\mu}{m_c}\right)^{3/2} \frac{1}{n_0(k_B T_e)^{3/2}} \frac{(\hbar\omega - E_G)^{1/2}}{\hbar\omega} e^{-\mu(\hbar\omega - E_G)/m_c k_B T_e}, \tag{2}$$

where μ is the reduced effective mass, $\mu = m_c m_v/(m_c + m_v)$, and m_c and m_v are the conduction- and valence-band effective masses, respectively. The solid curve in Fig. 3 is obtained from Eq. (2) with the bandgap energy of sample B, $E_G \sim 0.65$ eV, the temperature of electrons $T_e \sim 1100$ K, the effective mass ratio $\mu/m_c \approx 0.84$, and the proportional constant A is calculated by using the relevant parameters of InN.[3] The agreement between theory and experiment in Fig. 3 is good in overall magnitude near the bandgap. The

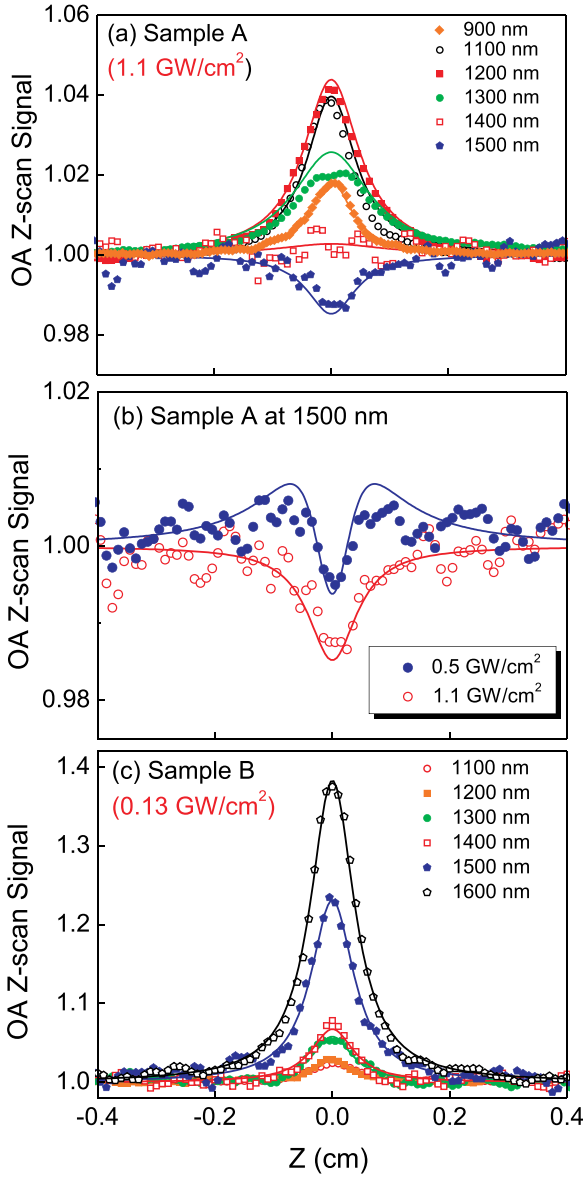

FIG. 2. (a) The excitation wavelength-dependent OA Z-scan curves of sample A measured at $I = 1.1\,\mathrm{GW/cm^2}$. (b) The OA Z-scan signals of sample A near the bandgap energy, excited at different intensities. While the one measured at $1.1\,\mathrm{GW/cm^2}$ only shows the RSA behavior, the signal measured at $0.5\,\mathrm{GW/cm^2}$ exhibits the transition from SA to RSA. (c) The excitation wavelength-dependent OA Z-scan curves of sample B measured at $I = 0.13\,\mathrm{GW/cm^2}$.

slight discrepancy at short wavelengths may be due to the restrictions of the band-filling model; $|\hbar\omega - E_G| \ll E_G$ and $k_BT \ll E_G$.[18] The values of σ measured by Tsai *et al.* (diamond symbols in Fig. 3) also show a good agreement with our results.

Meanwhile, the nonlinear absorption of sample A in Figs. 2(a) and 2(b) illustrates the evolution of nonlinear absorption from SA into RSA with the increase of λ and I_0, respectively. Similar SA-to-RSA switching near the bandgap has been reported for other materials,[19–21] and for GaN and nanocrystalline silicon, the origin of this transitional behavior is proposed to be the nonlinear absorption in exponential band-tail states below the conduction band.[21,22] Upon absorption of a photon with the energy just below the bandgap, the band-tail states may be saturated first and as the

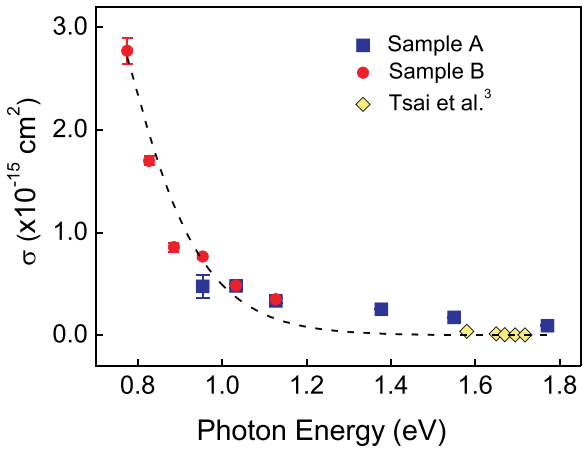

FIG. 3. The nonlinear absorption cross-section σ calculated from the OA Z-scan curves in Fig. 2. The results of Tsai *et al.*[3] (diamond symbols) are shown for comparison. The solid curve is obtained from Eq. (2), which is based on the band-filling effect.

sample approaches $z = 0$, the RSA due to either free-carrier absorption (FCA) or two-photon absorption (TPA) gradually dominates over SA. This intermediate absorption process is clearly observed in the Z-scan curve measured at $0.5\,\mathrm{GW/cm^2}$ [Fig. 2(b)]. With the absorption of photons further below the bandgap energy or the absorption at higher irradiance intensity, RSA becomes dominant. Since the SA-to-RSA transition is observed within the 1300 nm–1500-nm wavelength range, we can estimate the width of band-tail in sample A to be as large as 100 meV. This result is consistent with the previous reports on significant change of conduction band structure due to bandgap renormalization[16,23] and more significant near-band-edge shift due to the in-plane strain in *a*-plane InN film.[24]

The fitting result in Fig. 2(b) displays that the NLA coefficient upon RSA, β is $4.75 \times 10^{-6}\,\mathrm{cm/W}$ at 1500 nm. Similarly large value of β ($=3.65 \times 10^{-6}\,\mathrm{cm/W}$) was reported for $InN/In_{0.8}Ga_{0.2}N$ multiple-quantum-well at 1550 nm.[10] Recently, two-photon absorption coefficient of $1.67 \times 10^{-7}\,\mathrm{cm/W}$ was reported for InN layers ($E_G \sim 1.74\,\mathrm{eV}$) deposited by RF sputtering.[12] The discrepancy, in comparison with our result, may be due to the difference in the growth condition and the crystalline quality of the samples, on which the nonlinear properties of materials depend sensitively.

High intensity irradiance also induces a change in refractive index, which can be described by $n = n_0 + n_2 I$ with the nonlinear refractive index n_2. The measurement of n_2 is achieved by using the close-aperture (CA) Z-scan measurement.[13] The OA Z-scan measurement is sensitive to nonlinear absorption, whereas the CA Z-scan measurement exhibits features due to both nonlinear absorption and nonlinear refraction. Therefore, the information of nonlinear refraction alone is extracted by dividing the OA Z-scan signals by the CA Z-scan ones. Figure 4(a) illustrates the typical CA Z-scan profiles of samples A and B measured at $\lambda = 1300\,\mathrm{nm}$. Both samples show the valley followed by peak in the normalized transmittance data, suggesting that the samples possess self-focusing behavior with a positive n_2. The similar self-focusing behavior is observed for each sample over the whole tuning spectral range. With the assumption of a Gaussian profile for the laser beam, the

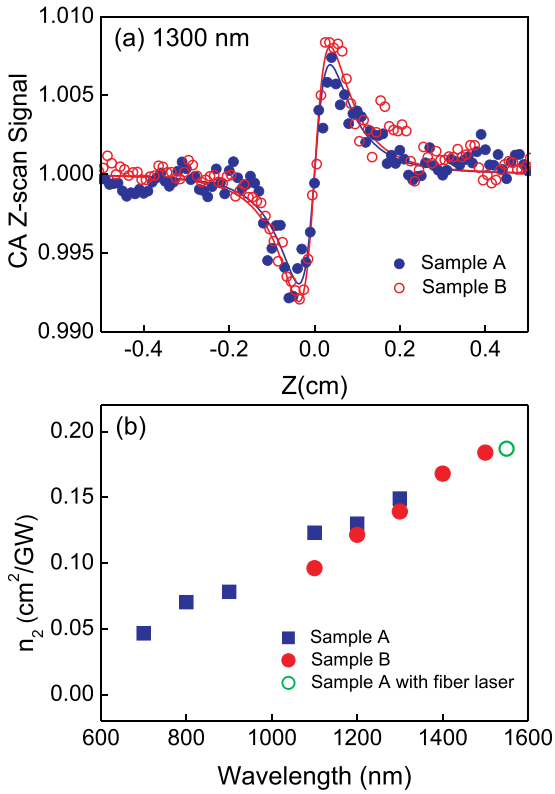

FIG. 4. (a) The CA Z-scan signals of samples A and B measured at 1300 nm, which exhibit the valley-peak dependence on the variation of z. (b) The spectral dependence of the nonlinear index of refraction calculated from the CA Z-scan signal at each wavelength. Green symbol corresponds to the nonlinear index of refraction measured by a femtosecond fiber laser.

variation of the on-axis sample transmittance in the far field is proportional to the phase shift

$$\Delta\phi = \frac{2\pi}{\lambda} L_{eff} n_2 I_0. \tag{3}$$

In a Kerr-like media, the refractive index $n(r)$ has the same radial profile as the laser $I(r)$ and then the difference between the normalized peak and valley transmittance, ΔT_{p-v} and the peak-to-valley separation in z are given by[13]

$$\Delta T_{p-v} = 0.406\Delta\phi, \quad \Delta z_{p-v} = 1.7 z_0. \tag{4}$$

The values of n_2 can be extracted from the fittings of the CA Z-scan curves by using Eqs. (3) and (4). Figure 4(b) shows the calculated wavelength-dependent n_2, which increases from 4.9×10^{-11} to 1.9×10^{-10} cm^2/W as the wavelength increases from 700 nm to 1500 nm. Another value of n_2 measured by using a femtosecond fiber laser ($\lambda = 1550$ nm) is also plotted for comparison.

In summary, comprehensive nonlinear optical properties of InN epilayers were measured by the femtosecond Z-scan technique. For resonant excitation near the bandgap energy, the nonlinear absorption in InN can be described by the saturated absorption based on the band-filling effect and the corresponding nonlinear optical absorption cross-sections were estimated in a wavelength range of 700–1500 nm. From the spectral dependence of OA Z-scan signals near the bandgap energy, the SA-to-RSA transition due to the competition between SA in band-tail states and two-photon-related RSA is observed. When excited With below bandgap excitation, the RSA process becomes dominant and the estimated RSA coefficient is 4.75×10^{-6} cm/W. From the CA Z-scan measurement, the nonlinear refraction indices are estimated of the order of 10^{-10} cm^2/W. Our results identify InN as a promising yet unexplored material for ultrafast nonlinear optical devices and its large nonlinearity can enable such applications as all-optical switching, logic, and wavelength conversion.

The authors would like to thank Professor S. Gwo of National Tsing Hua University in Taiwan for providing the InN films. This work was supported by the National Science Council (Grant No. NSC-101-2112-M-009-MY3 and the Science Vanguard Research Program, Grant No. NSC-102-2628-M-007-001) in Taiwan.

[1]V. Yu. Davydov, A. A. Klochikhin, R. P. Seisyan, V. V. Emtsev, S. V. Ivanov, F. Bechstedt, J. Furthmüller, H. Harima, A. V. Mudryi, J. Aderhold, O. Semchinova, and J. Graul, Phys. Status Solidi B **229**, R1 (2002).
[2]A. G. Bhuiyan, A. Hashimoto, and A. Yamamoto, J. Appl. Phys. **94**, 2779 (2003).
[3]S. K. O'Leary, B. E. Foutz, M. S. Shur, U. V. Bhapkar, and L. F. Eastman, J. Appl. Phys. **83**, 826 (1998).
[4]B. E. Foutz, S. K. O'Leary, M. S. Shur, and L. F. Eastman, J. Appl. Phys. **85**, 7727 (1999).
[5]K. T. Tsen, C. Poweleit, D. K. Ferry, H. Lu, and W. J. Schaff, Appl. Phys. Lett. **86**, 222103 (2005).
[6]C. Honsberg, O. Jani, A. Doolittle, E. Trybus, G. Namkoong, I. Ferguson, D. Nicole, and A. Payne, in *Proceedings of European Photovoltaic Solar Energy Conference* (2004), Vol. 15, pp. 7–11.
[7]H. Ahn, C.-C. Yu, P. Yu, J. Tang, Y.-L. Hong, and S. Gwo, Opt. Express **20**, 769 (2012).
[8]Z. Q. Zhang, W. Q. He, C. M. Gu, W. Z. Shen, H. Ogawa, and Q. X. Guo, Appl. Phys. Lett. **91**, 221902 (2007).
[9]T.-R. Tsai, T.-H. Wu, J.-C. Liao, T.-H. Wei, H.-P. Chiang, J.-S. Hwang, D.-P. Tsai, and Y.-F. Chen, J. Appl. Phys. **105**, 066101 (2009).
[10]F. B. Naranjo, P. K. Kandaswamy, S. Valdueza-Felip, V. Calvo, M. González-Herráez, S. Martin-Lopéz, P. Corredera, J. A. Méndez, G. R. Mutta, B. Lacroix, P. Ruterana, and E. Monroy, Appl. Phys. Lett. **98**, 031902 (2011).
[11]F. B. Naranjo, M. González-Herráez, H. Fernández, J. Solis, and E. Monroy, Appl. Phys. Lett. **90**, 091903 (2007).
[12]S. Valdueza-Felip, L. Monteagudo-Lerma, J. Mangeney, M. González-Herráez, F. H. Julien, and F. B. Naranjo, IEEE Photon. Technol. Lett. **24**, 1998 (2012).
[13]M. Sheik-Bahae, A. A. Said, T. H. Wei, D. J. Hagan, and E. W. Van Stryland, IEEE J. Quantum Electron. **26**, 760 (1990).
[14]H. Ahn, Y.-P. Ku, C.-H. Chuang, C.-L. Pan, H.-W. Lin, Y.-L. Hong, and S. Gwo, Appl. Phys. Lett. **92**, 102103 (2008).
[15]H. Ahn, C.-H. Shen, C.-L. Wu, and S. Gwo, Appl. Phys. Lett. **86**, 201905 (2005).
[16]J. Wu, W. Walukiewicz, W. Shan, K. M. Yu, J. W. Ager III, E. E. Haller, H. Lu, and W. J. Schaff, Phys. Rev. B **66**, 201403 (2002).
[17]B. L. Justus, A. L. Huston, and A. J. Campillo, App. Phy. Lett. **63**, 1483 (1993).
[18]D. A. B. Miller, C. T. Seaton, M. E. Prise, and S. D. Smith, Phys. Rev. Lett. **47**, 197 (1981).
[19]R. Rangel-Rojo, S. Yamada, H. Matsuda, and D. Yankelevich, Appl. Phys. Lett. **72**, 1021 (1998).
[20]K. Unnikrishnan, J. Thomas, V. Nampoori, and C. Vallabhan, Appl. Phys. B **75**, 871 (2002).
[21]Y. L. Huang, C. K. Sun, J. C. Liang, S. Keller, M. P. Mack, U. K. Mishra, and S. P. DenBaars, Appl. Phys. Lett. **75**, 3524 (1999).
[22]Y. J. Ma, J. I. Oh, D. Q. Zheng, W. A. Su, and W. Z. Shen, Opt. Lett. **36**, 3431 (2011).
[23]A. Kasic, E. Valcheva, B. Monemar, H. Lu, and W. J. Schaff, Phys. Rev. B **70**, 115217 (2004).
[24]Y. Li, R. Zhang, B. Liu, Z. Xie, D. Fu, H. Su, and Y. Zheng, J. Appl. Phys. **110**, 033105 (2011).